Roberts, J. W., & Devoret, R. (1983) in *Lambda II* (Hendrix, R. W., Roberts, J. W., Stahl, F. W., & Weisberg, R. A., Eds.) pp 123–144, Cold Spring Harbor Laboratory, Cold Spring Harbor, NY.
Rupley, J. A., Gratton, E., & Careri, G. (1983) *Trends Biochem. Sci. (Pers. Ed.) 8*, 18–22.
Sauer, R. T. (1978) *Nature (London) 276*, 301–302.
Sauer, R. T. (1979) Ph.D. Thesis, Harvard University.
Sauer, R. T., Ross, M. J., & Ptashne, M. (1982a) *J. Biol. Chem. 257*, 4458–4462.
Sauer, R. T., Yocum, R. R., Doolittle, R. F., & Pabo, C. O. (1982b) *Nature (London) 298*, 447–451.
Schnarr, M., Pouyet, J., Granger-Schnarr, M., & Daune, M. (1985) *Biochemistry 24*, 2812–2818.
Sharp, P. A. (1985) *Cell (Cambridge, Mass.) 42*, 397–400.
Shea, M. A., & Ackers, G. K. (1985) *J. Mol. Biol. 181*, 211–230.
Stroynowski, I., van Cleemput, M., & Yanofsky, C. (1982) *Nature (London) 298*, 38–41.
Tomizawa, J.-I., & Som, T. (1984) *Cell (Cambridge, Mass.) 38*, 871–878.
Walker, G. C. (1984) *Microbiol. Rev. 48*, 60–93.
Zaug, A. J., & Cech, T. R. (1985) *Science (Washington, D.C.) 229*, 1060–1064.
Zaug, A. J., & Cech, T. R. (1986) *Science (Washington, D.C.) 231*, 470–475.
Zaug, A. J., Grabowski, P. J., & Cech, T. R. (1983) *Nature (London) 301*, 578–583.

DNA Cleavage Specificity of a Group of Cationic Metalloporphyrins†

Brian Ward, Andrew Skorobogaty,‡ and James C. Dabrowiak*
Department of Chemistry, Syracuse University, Syracuse, New York 13244-1200
Received April 16, 1986; Revised Manuscript Received July 14, 1986

ABSTRACT: The ability of a group of water-soluble metalloporphyrins to cleave DNA has been investigated. Incubation of Mn^{3+}, Fe^{3+}, or Co^{3+} complexes of *meso*-tetrakis(*N*-methyl-4-pyridiniumyl)porphine (H_2T4MPyP) with DNA in the presence of ascorbate, superoxide ion, or iodosobenzene results in DNA breakage. Comparisons between the rates of porphyrin autodestruction with the rates of strand scission of covalently closed circular PM2 DNA indicate that the porphyrins remain intact during the cleavage process. Analysis of the porphyrin-mediated strand scissions on a 139-base-pair restriction fragment of pBR322 DNA using gel electrophoresis/autoradiography/microdensitometry reveals that the minimum porphyrin cleavage site is $(A{\cdot}T)_3$. The cleavage pattern within a given site was found to be asymmetric, indicating that porphyrin binding and the strand scission process are highly directional in nature. In addition to an analysis of the mechanism of porphyrin-mediated strand breakage in terms of the DNA cleavage mechanism of methidium–propyl–iron–EDTA and Fe–bleomycin, the potential of the cationic metalloporphyrins as footprinting probes and as new "reporter ligands" for DNA is presented and discussed.

The interaction of metal ions with DNA is of considerable current interest (Eichhorn, 1973; Eichhorn & Marzilli, 1982; Barton, 1985). In addition to simple aquated metal salts, several complexes containing a variety of different coordinated ligands are known to interact with DNA. For example, the exchange-inert metal complex $[Co(NH_3)_6]^{3+}$ has been shown to be an effective inducing agent for stabilizing left-hand helical DNA, termed Z-DNA, (Behe & Felsenfeld, 1981). X-ray crystallographic studies have indicated that the compound exerts its effects through electrostatic and hydrogen-bonding interactions to groups located in the major groove of DNA (Gessner et al., 1985). In addition to $[Co(NH_3)_6]^{3+}$, compounds of Cu^{2+}, Zn^{2+}, and Co^{3+} having multidentate amine type ligands have been found useful in studies of DNA conformation (Barton, 1985; Fazakerly, 1984; Woisard, et al. 1985). The exchange-inert complex ion tris(4,7-diphenylphenanthroline)cobalt(III) is especially noteworthy in this regard since the two enantiomers of the cation bind to DNA with different apparent affinities. Furthermore, the compound can be photoactivated to produce strand scission, thus clearly identifying the regions of Z-conformation in DNA (Barton & Raphael, 1985).

Nuclease activity also can be elicited from the complex ion bis(*o*-phenanthroline)copper(I), (Spassky & Sigman, 1985). Recent studies of this cation with wild-type, Ps, and L8-UV-5 *lac* promoters have suggested that the compound is sensitive to sequence-dependent structural changes in DNA.

One of the most versatile metal-containing agents for studying drug–DNA interactions is the synthetic DNA cleaving agent methidium–propyl–iron–EDTA, MPE (Van Dyke et al., 1982). This compound, which contains an iron–EDTA moiety tethered to a methidium group, has been used in footprinting studies to uncover the binding sequence specificities of a number of anticancer drugs and other ligands capable of equilibrium binding to DNA. The success of the compound as a footprinting probe is related to the fact that it can bind to DNA via intercalation and at the same time produce a flux of DNA-damaging radicals through reductive activation of the tethered iron–EDTA moiety. In addition to attachment to methidium, the iron–EDTA group also has been tethered to a number of *N*-methylpyrrole oligopeptides. The strand scission sites produced by these modified oligopeptides on defined-sequence DNA have provided valuable information on the manner in which naturally occurring groove-binding peptides such as netropsin and distamycin are able to "read"

† This work was supported by grants from the National Institutes of Health (GM31895) and the American Cancer Society (CH-296).
‡ Present address: Department of Biochemistry, La Trobe University, Bundoora, Victoria, Australia 3083.

0006-2960/86/0425-6875$01.50/0

DNA sequence (Schultz & Dervan, 1984).

Recent investigations with the metal complexes of the water soluble tetracationic porphyrin *meso*-tetrakis(*N*-methyl-4-pyridiniumyl)porphine (H_2T4MPyP) (Fiel et al., 1985; Pasternack et al., 1984; Kelly et al., 1985) have shown that these compounds can also bind to DNA. Furthermore, it has been established that the mode of porphyrin binding to DNA is dramatically affected by ligand structure and/or metal coordination geometry. Both outside binding and intercalation are thought to occur in the binding process. These facts, coupled with the observations that the compounds can be chemically and photochemically activated to produce DNA strand scission (Fiel et al., 1982; Kelly et al., 1985), underscore the potential importance of the complexes as probes of DNA structure and as new agents in studying drug–DNA interactions by using footprinting methodology (Lane et al., 1983; Lane et al., 1985; Van Dyke et al., 1982).

In a previous paper (Ward et al., 1986) we examined the binding sequence specificity of M–T4MPyP, where M is Mn^{3+}, Fe^{3+}, Co^{3+}, Ni^{2+}, Cu^{2+}, and Zn^{2+}, using DNase I footprinting methology. The outside binding porphyrins, Mn–, Fe–, Co–,

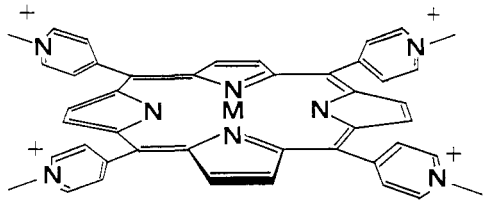

M-T4MPyP

M:Mn,Fe,Co

and Zn–T4MPyP, were found to bind to AT-rich regions of a 139-base-pair restriction fragment of pBR322 DNA while Ni– and Cu–T4MPyP were observed to interact at both AT and GC sites of the fragment. In this report we show that it is possible to chemically activate Mn^{3+}–, Fe^{3+}–, and Co^{3+}–T4MPyP by using three different activating agents and to produce porphyrin-mediated DNA strand scission. Electrophoresis studies with PM2-DNA and optical measurements indicate that the porphyrin remains largely entact during the strand breakage process. Furthermore, examination of the site of cleavage on a 139-base-pair restriction fragment of pBR322 DNA by using high-resolution gel electrophoresis and autoradiography/microdensitometry (Dabrowiak et al., 1986) reveal that the smallest porphyrin cleavage sites have AT sequences and are three nucleotides in length. In addition, DNA breakage by the porphyrins at a given site is found to be asymmetric in nature, yielding a cleavage pattern unlike agents containing a tethered iron–EDTA group (Schultz & Dervan, 1984).

Materials and Methods

The Mn^{3+}, Fe^{3+}, and Co^{3+} complexes of H_2T4MPyP were prepared as previously published (Pasternack et al., 1983a). Concentrations of the metalloporphyrins in aqueous solution were measured by using published extinction coefficients (Pasternack et al., 1983b). Bleomycin (Blenoxane) was a gift from Bristol-Myers, Syracuse, NY. The Fe^{3+}–bleomycin complex was formed by mixing equimolar quantities of $FeCl_3 \cdot 6H_2O$ and bleomycin at pH 7.0. Concentrations of the antibiotic were determined by using $\epsilon_{M(290)} = 15\,100\ M^{-1}\ cm^{-1}$ (Dabrowiak, 1982).

Calf thymus DNA (Sigma) was deproteinized by extraction with phenol and 24:1 chloroform–isoamyl alcohol (Maniatis, 1982). Bacteriophage PM2 (Boehringer Mannheim) was used without further deproteinization but was dialyzed extensively against 50 mM Tris–HCl and 20 mM EDTA, pH 7.0, and finally against 50 mM Tris–HCl and 1 mM EDTA, pH 7.0. In experiments involving bleomycin, DNA solutions were kept in 50 mM Tris–HCl, pH 7.0.

Reactions Involving PM2 DNA. Digestion of PM2 DNA with Mn^{3+}–, Fe^{3+}–, and Co^{3+}–T4MPyP was carried out at 37 °C for 20 min in 50 mM Tris–HCl/1 mM EDTA, pH 7.0, buffer. Ten microliters of the DNA (50 μM in base pairs) and porphyrin at porphyrin to DNA ratios, r_t, of 0.05 and 0.005 were allowed to equilibrate for 30 min prior to addition of activator. Initiation of the cleavage reaction was accomplished upon addition of 5 μL of a 15 mM solution of either ascorbic acid, potassium superoxide, or iodosobenzene to the DNA–porphyrin solution, the latter of which was in 30% methanol/buffer. Potassium superoxide solutions were made at 0 °C immediately prior to their use. Experiments involving $MnCl_2$, $FeCl_3$, $CoCl_2$ or Fe–bleomycin were carried out in an analogous fashion.

For reaction termination and analysis, the reaction mixtures were loaded into the wells of a 0.8% horizontal agarose gel with the current on and electrophoresed at 1 V/cm for 14 h in 80 mM Tris–phosphate, 2 mM EDTA pH 7.0 buffer. The gels were subsequently stained with ethidium bromide and photographed by using established procedures (Maniatis et al., 1982). Photographic negatives of the stained agarose gels were scanned by employing the computer-densitometric system described elsewhere (Dabrowiak et al., 1986). Calibration involving various amounts of PM2 DNA revealed that the scanned cross sectional area of a band on the negative was proportional to the concentration of stained form I DNA in the gel.

Reactions Involving Calf Thymus DNA. Porphyrin degradation induced by the addition of ascorbate, superoxide, or iodosobenzene (5.0 mM) was monitored spectrally between 300 and 700 nm in the presence of calf thymus DNA, r_t of 0.05, 0.25 mM base pairs. The porphyrin absorption spectrum was recorded, the monochrometer was set to the Soret band absorbance, activator was added, and the Soret band intensity was monitored as a function of time. Where spectral changes were slow, the absorption spectrum was scanned. In each case the final absorption spectrum, 20 min after the addition of activator, was recorded.

Porphyrin strand scission of calf thymus DNA under the above conditions was analyzed for base propenals by using the thiobarituric acid assay (Giloni et al., 1981). As a control, iron bleomycin was also examined.

Reactions Involving the HindIII–NciI Restriction Fragment of pBR322. The restriction fragment was 3′-end labeled by filling in an A at position 33 of the fragment by using [α-^{32}P]dATP and reverse transcriptase (Lown et al., 1986a). The numbering index of the fragment is the same as the genomic numbering system for PBR322 DNA (Maniatis et al., 1982). Checks using denaturing gel electrophoresis revealed that the fragment had not sustained cleavage during the labeling and isolation procedures.

The fragment degradation experiments with the porphyrins were carried out in a 50 mM Tris–HCl/0.1 mM EDTA pH 7.0 buffer. The 8-μL reaction mixtures consisted of buffered solutions of 2 μL of sonicated calf thymus DNA (770 μM base pairs); 2 μL of fragment (~7 μM), 2 μL of buffer (control) or porphyrin, and 2 μL of activating agent (20 mM). The values of r_t studied were in the range $0 \leq r_t \leq 0.25$.

After addition of the porphyrin but prior to addition of activating agent, the solutions containing the porphyrin and

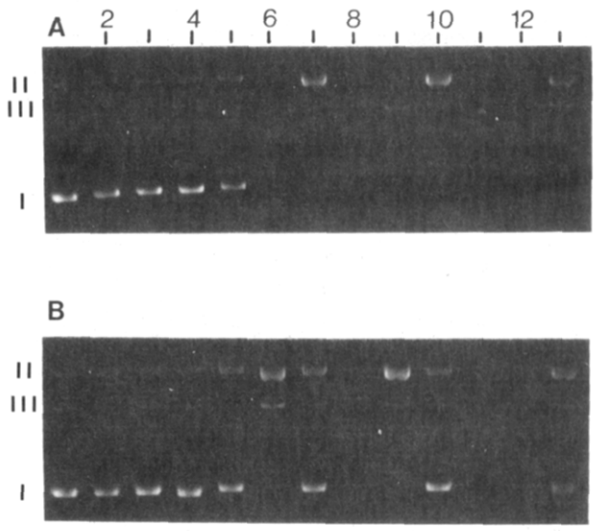

FIGURE 1: Strand scission of PM2 DNA by the metalloporphyrins. The DNA was electrophoresed on an agarose gel and treated as described in the experimental section. Gels A and B involved porphyrin to DNA-base-pair ratios of 0.05 and 0.005 respectively. Lane assignments: 1A,B, DNA control; 2A, Mn–(T4MPyP) control; 3A, Fe–(T4MPyP) control; 4A, Co–(T4MPyP) control; 2B, ascorbate control; 3B, KO_2 control; 4B, iodosobenzene control; 5A,B, Mn–(T4MPyP) + ascorbate; 6A,B Fe–(T4MPyP) + ascorbate; 7A,B, Co–(T4MPyP) + ascorbate; 8A,B, Mn–(T4MPyP) + KO_2; 9A,B, Fe–(T4MPyP) + KO_2; 10A,B, Co–(T4MPyP) + KO_2; 11A,B, Mn–(T4MPyP) + iodosobenzene; 12A,B, Fe–(T4MPyP) + iodosobenzene; 13A,B, Co–(T4MPyP) + iodosobenzene. The various forms of PM2 DNA—covalently closed circular, form I, nicked circular, form II, and linear, form III—are indicated in the figure.

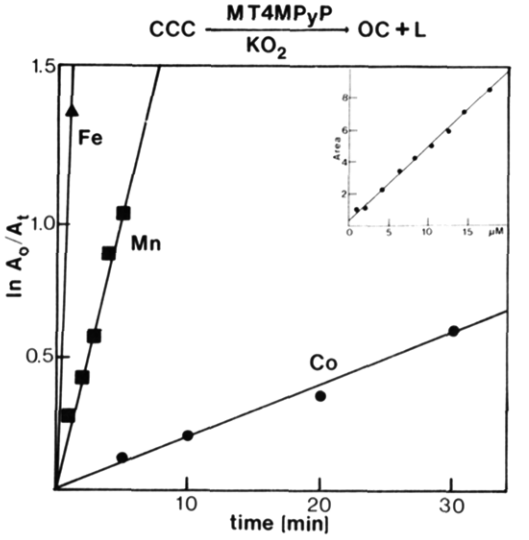

FIGURE 2: Rate disappearance plots (based on a single determination) of closed circular PM2 DNA as a result of incubation with M–T4MPyP + KO_2 (M = Mn, Fe, Co). Inset: Calibration of area vs. concentration in base pairs of closed circular PM2 DNA. A_0 = area at $t = 0$; A_t = area at time t.

DNA were allowed to equilibrate for 30 min. After 20 min at 37 °C, 10 μL of a solution containing 70% aqueous urea, 20 mM EDTA, and 0.025% each of bromphenol blue and xylene cyanol was added, followed by heating to 80 °C for 10 min.

Electrophoresis, autoradiography, and microdensitometry were carried out as described previously (Dabrowiak, et al., 1986; Ward et al., 1986). The maximum optical density of the analyzed bands was <1.0. The size of the "bar" on the histograms presented is proportional to the maximum optical density derived from linear scanning through the band (nucleotide) in question. Due to poor separation of the longer labeled oligomers in the gel the cleavage sites (±1 BP) and intensities for positions >~110 of the fragment have been estimated. Establisment of sequence was by reference to the known cleavage pattern of the fragment in the presence of DNase I (Lown et al., 1986a).

Results

Incubation of the covalently closed circular form of PM2 DNA (form I) with an agent capable of producing DNA strand scission results in the conversion of form I DNA into a nicked circular form (form II), which, after additionial cleavage, reverts to a linear form of the phage DNA (form III). The results of the PM2 DNA degradation experiments with the metalloporphyrins are shown in Figures 1 and 2, and the half-life data are presented in Table I. As is evident from the inset of Figure 2, calibration experiments involving scanning of the photographic negative yielded areas proportional to the amount of ethidium bromide stained covalently closed circular (form I) PM2 DNA present in the agarose gel. Plots of ln (A_t/A_0), where A_0 is the area of form I DNA at $t = 0$ and A_t is the corresponding area at a time after the initiation of the digest with a porphyrin/activator combination, vs. time were linear except for Co–T4MPyP in the presence of ascorbate. Although plots of the latter (data not shown) were linear in the initial stages of the digestion, $0 < t < \sim 20$ min, they were found to deviate from linearity at $t > \sim 20$ min. Table I shows that the rates of the various combinations in degrading PM2 DNA are in the order Fe (all activators), Mn (iodosobenzene) >> Mn (superoxide), Co (iodosobenzene) > Co (ascorbate) > Co (superoxide) > Mn (ascorbate). The relative overall ability of the three metalloporphyrins to degrade PM2 DNA under the conditions employed is Fe >> Co > Mn for ascorbate while for superoxide and iodosobenzene the order is Mn > Fe > Co.

Table I: Approximate Half-Lives of Form I PM2 DNA Disappearance (min)[a]

activating agent	Mn–T4MPyP	Fe–T4MPyP	Co–T4MPyP
ascorbate	54	≪1	14
superoxide	3	≪1 (1)[b]	34
iodosobenzene	≪1	≪1 (10)[b]	3

[a] The digestion conditions were as described under Materials and Methods: $r_t = 0.002$, porphyrin to PM2 DNA base pairs; [activator] = 5.0 mM. [b] Approximate half-life for Fe–T4MPyP in the presence of calf thymus DNA: r_t 0.05; [activator], 5.0 mM; [DNA–BP], 0.25 mM. The observed porphyrin half-lives for all other porphyrin-activator combinations were ≫2 h. The figures given in the table are based on a single determination.

To ascertain whether possible degradation products of the porphyrins were responsible for the observed nuclease activity, the optical spectra of the metalloporphyrins, in the Soret region, were monitored as a function of time in the presence of calf thymus DNA. In the case of Fe–T4MPyP in the presence of superoxide or iodosobenzene a decrease in intensity of the porphrinoid absorption spectrum was observed with time. The half-lives for the observed intensity decreases, assumed to be porphyrin autodestruction (Traylor et al., 1984), were ~1 and ~10 min, respectively (Table I). In all other cases activation produced rapid modification in the initial porphyrin absorption spectrum, to a new one that was either invariant with time or decreased in intensity with a long half-life, >>2 h. A check on the ability of the free metal ions alone, possible degradation products from the metalloporphyrins, to cause DNA strand scission in the presence of ascorbate, superoxide, or iodosobenzene was made. With the exception of $FeCl_3$ + ascorbate none of the other reaction conditions initiated observable

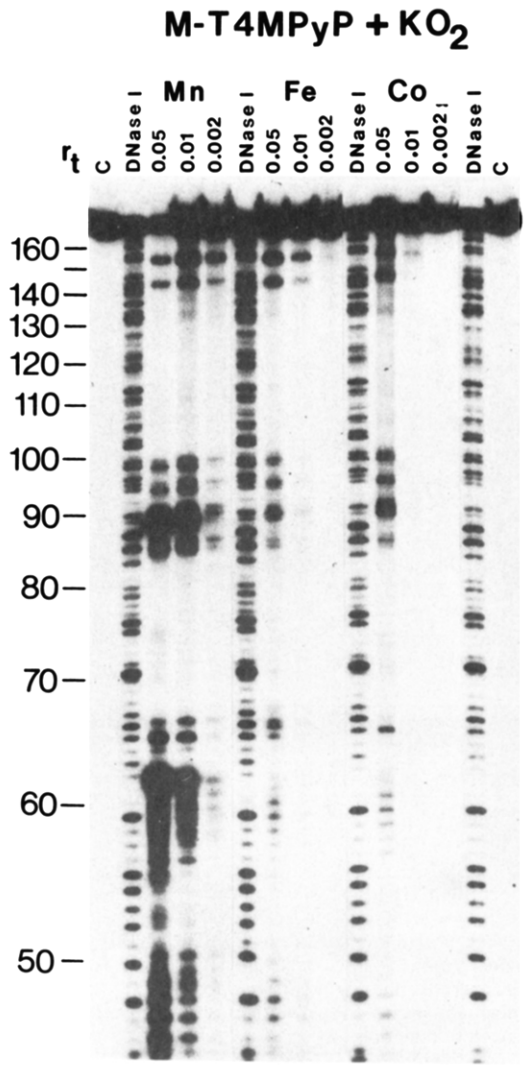

FIGURE 3: Autoradiogram of M–T4MPyP + KO_2 digestion, where M is Fe, Co, or Mn, of the 139-base-pair fragment of pBR322 DNA. Lanes marked C are no porphyrin or DNase I. Lanes marked DNase I are DNase I digested fragment in the absence of porphyrin. The porphyrin to DNA base-pair ratios for the various porphyrins are given above the lanes.

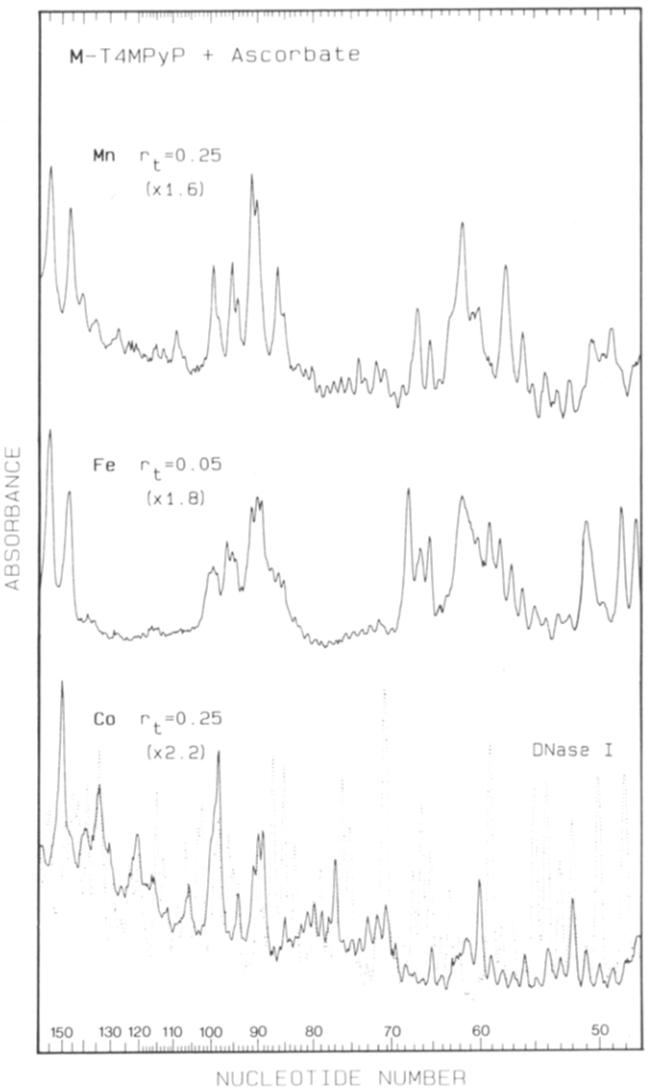

FIGURE 4: Densitometric traces of strand scission reactions of M–T4MPyP + ascorbate with the 139-base-pair restriction fragment from pBR322. The dotted trace is the DNase I digest of the fragment. Numbers in parentheses are absorbance scaling factors relative to DNase I.

amounts of PM2 DNA strand scission. In the case of $FeCl_3$ + ascorbate the amount of strand scission relative to Fe–T4MPyP and ascorbate was less than 10%.

An autoradiogram showing the porphyrin-induced cleavage of the restriction fragment in the presence of superoxide is shown in Figure 3. The densitometric scans resulting from experiments with all of the porphyrin-activator combinations studied are shown in Figures 4–6. The observed sites of cleavage on the sequence of the 139-mer are given in Figures 7–9.

For Fe–T4MPyP, which yields similar cleavage patterns in the presence of any of the three activators, the most intense sites of breakage occur at positions 46–50, 55–62, 66–68, 85–87, 89–92, 94–96, and 98–100. These regions of cleavage are essentially the same as the porphyrin binding sites uncovered using DNAse I footprinting methology (Ward et al., 1986). However, footprinting revealed only long (15 nucleotides) inhibitions in these regions, while inspection of the porphyrin cleavage patterns shows well-defined AT sites with a minium length of three nucleotides, bordered by a G·C base pair. In the GC-rich region of the fragment, positions 101–173, a limited number of cleavages were observed and then only at AT sequences, positions ~136 (weak), ~147, and ~158. Although porphyrin-mediated strand scission took place at all of the four possible bases of DNA, the most often cleaved sites were A and T.

The electrophoretic mobilities of the shortest analyzed oligomers, 14–15-mers, for all porphyrin and all conditions of activation appeared to be identical with those of their DNase I produced counterparts. However certain bands were found between the bands of the DNase I "ladder" at positions 50 (A), 61 (A), 66 (T), 67 (T), and 90 (T). As is evident from the autoradiogram shown in Figure 3, these bands appear to increase in intensity relative to the other bands as the extent of cleavage increases.

The cleavage patterns of Co– and Mn–T4MPyP are qualitatively similar to those of Fe–T4MPyP. In the case of Mn–T4MPyP clear separation between the close lying AT binding sites can be observed (Figure 7). Activation with iodosobenzene produces only limited breakage sites (all 5′ → 3′) TTA (67–65), ATA (87–85), TTA (96–94), ATT (100–98), and TAT (148–146). Larger sites with strong cleavage are ATAAA (50–46), AATTTAA (62–56), ATTT (92–89), and ATAA (159–156). Interestingly, these compounds also produce weak cleavage in the presence of ascorbate and iodosobenzene in the GC-rich region, 69–81. Due to the

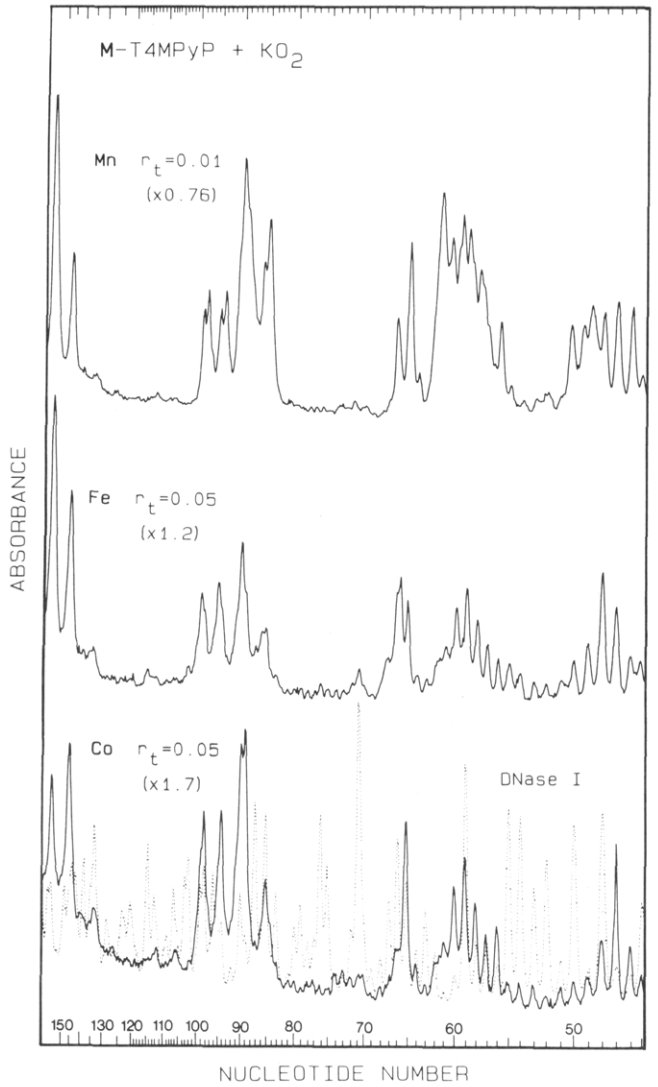

FIGURE 5: Densitometric traces of strand scission reactions of M–T4MPyP + KO_2 with the 139-base-pair restriction fragment form pBR322. The dotted trace is the DNase I digest of the fragment. Number in parentheses are absorbance scaling factors relative to DNase I.

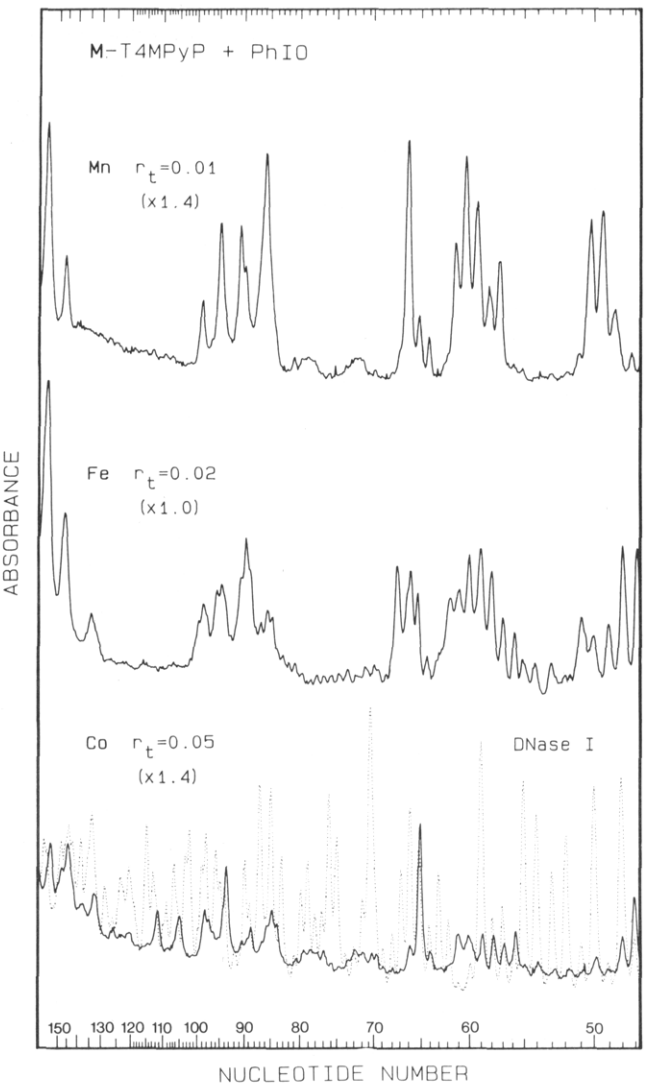

FIGURE 6: Densitometric traces of strand scission reactions of MT4MPyP + iodosobenzene with the 139-base-pair fragment from pBR322. The dotted trace is the DNase I digest of the fragment. Numbers in parentheses are absorbance scaling factors relative to DNase I.

slow DNA cleavage rate by these compounds in the presence of ascorbate, digests were carried out at a value of r_t (0.25) greater than those used for all other porphyrin-activator combinations. As with Fe–T4MPyP the electrophoretic mobilities of the shortest fragments using any of the porphyrin-activator combinations for Mn– and Co–TMPyP were identical with those of their DNase I generated counterparts.

In order to ascertain if base 2 propenals were produced in the various porphyrin-mediated strand scission processes, assays with thiobarbituric acid were carried out. While the products from DNA damage by iron bleomycin showed the presence of base 2-propenals, parallel tests with the three metalloporphyrins using all three activating agents were negative.

Discussion

Porphyrin model compounds in the presence of various activating agents have been studied extensively as model systems for naturally occurring peroxidases (Peterson et al., 1973; Groves, 1979; Traylor et al., 1984a). Examination of the chemical events surrounding the activation process has revealed that both iron and manganese porphyrins can be oxidized by iodosobenzene or superoxide ion to high-valent metalloporphyrins possessing an axially ligated oxygen atom (Groves et al., 1983). These oxo species are exceedingly reactive and are capable of oxygen insertion into C—H and C=C bonds to form alcohols and epoxides (Groves & Nemo, 1983a,b). This process takes place by direct contact between the substrates, an alkane or olefin, with the oxygen atom located in the axial site of the high-valent metalloporphyrin. In the presence of excess activating agent the porphyrin can be reactivated, thus making the process catalytic.

In addition to using oxidizing agents, Mn^{3+} porphyrins can be activated by the reducing agent ascorbate in the presence of molecular oxygen. In this case, reduction to Mn^{2+} by ascorbate results in a complex which reacts with molecular oxygen to yield a high-valent species similar to that formed by Mn^{3+} porphyrin in the presence of superoxide ion or iodosobenzene (Fontecave & Mansuy, 1984). This complex is catalytically active and readily converts alkanes and olefins to alcohols and epoxides, respectively. Although relatively little is known about the reaction of the various activating agents with Co^{3+}–porphyrins, Co^{3+}–T4MPyP has been reported to exhibit superoxide dismutase activity (Peretz et al., 1982).

Equation 1 outlines the general mechanism by which the metalloporphyrins Co–, Mn–, and Fe–T4MPyP, are able to

FIGURE 7: Histogram of Mn–T4MPyP-mediated strand scission of the restriction fragment activated with ascorbate, KO_2, and iodosobenzene. The lengths of the bars are proportional to the absorption maximum of the densitometrically scanned peak appearing on the autoradiogram.

FIGURE 8: Histogram of Fe–T4MPyP-mediated strand scission of the restriction of fragment activated with ascorbate, KO_2, and iodosobenzene.

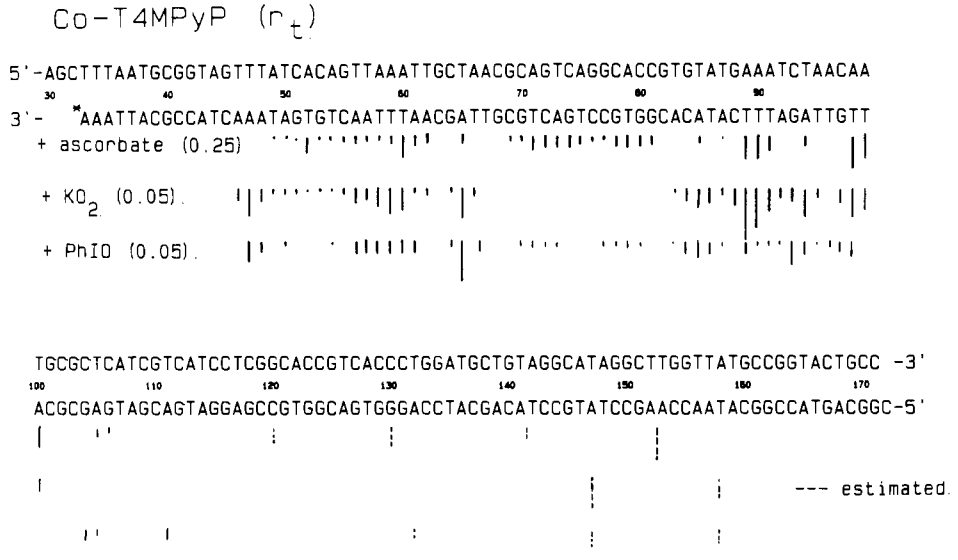

FIGURE 9: Histogram of Co–T4MPyP-mediated strand scission of the restriction fragment activated with ascorbate, KO_2, and iodosobenzene.

degrade DNA. Studies with PM2 DNA revealed that the rate

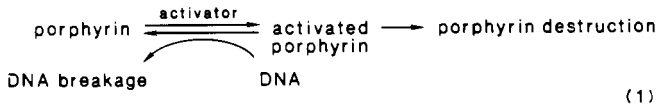

(1)

of porphyrin-mediated DNA breakage is dependent on both the nature of the activator present and the coordinated metal ion. As is evident from DNA cleavage rate data, activation by iodosobenzene is greatest for all three metalloporphyrins. This observation may be related to the fact that of the three activators iodosobenzene is the only one that is expected to react directly with the metalloporphyrins in a one-step process to yield the high-valent catalytically active species (Groves & Nemo, 1983a,b). The measured half-lives also show that Fe–T4MPyP under all conditions of activation cleaves DNA at the highest rate. Although this compound was observed to autodegrade in the presence of activator and DNA, the rate of autodestruction was found to be slower than the rate of DNA breakage (Figures 1 and 2; Table I). Thus, it appears that in this case, as well as for Mn–T4MPyP and Co–T4MPyP for which no autodestruction under the conditions of the experiment was observed, the porphyrins remain largely entact during the activation and strand scission processes. The DNA cleavage rate of Co–T4MPyP is the lowest of the three porphyrins studied. The reason for this is presently unknown but it may be due to the fact that Co^{3+} complexes are slow to substitute, a factor that may affect the activation step in the process (Harris & Toppen, 1978).

Interestingly, as assayed by agarose gel electrophoresis, Fe–T4MPyP has been reported to nick closed circular DNA in the absence of any added activating agent (Fiel et al., 1982). Control experiments involving polyacrylamide gel electrophoresis did not display this behavior. Following a 20 min incubation period at 37 °C, the Fe–T4MPyP·(PM2 DNA) was electrophoresed on agarose in the presence of an Fe^{2+} specific ligand, *n*-butyl isocyanide, in the loading buffer. No auto nicking was observed in the lane containing isonitrile. This observation shows that autocutting occurs only after the sample is loaded into the well of an agarose gel. It thus appears that components present in the agarose (reducing agents) are capable of activating Fe–T4MPyP.

As is evident from Figures 3–9, the metalloporphyrins cleave in AT-rich regions of DNA. While DNase I footprinting analyses (Ward et al., 1986) were unable to resolve individual porphyrin binding sites, the porphyrin cleavage pattern clearly shows the minimum size site is three nucleotides in length. This is most evident in the cleavage pattern of Mn– and Fe–T4MPyP (Figures 7 and 8). Interestingly, the region 85–101 of the fragment is actually composed of four close-lying porphyrin binding sites: three trinucleotide sites having the sequences (5′ → 3′) ATA, TTA, and ATT and a tetranucleotide site with the sequence ATTT. The minimum binding requirement of $(A{\cdot}T)_3$ is further exemplified by the cleavages that take place in the region 101–172. In this predominantly GC rich segment of the fragment, cleavage is observed at (5′ → 3′) TAT and ATAA. Although dinucleotide AT sequences occur a number of times throughout this regon, cleavage at these sites is infrequent.

On the basis of what is already known about the porphyrin binding mechanism and the structure of DNA, certain aspects of the porphyrin–DNA interaction can be uncovered. Opposite strand DNase I footprinting analysis reveals that porphyrin binding takes place in the minor groove of DNA (Ward et al., 1986). Since the compounds possess high cationic charge and, with the exception of the axial ligands, are devoid of hydrogen bond donor/acceptor capacity, their interaction with DNA appears to be largely electrostatic in nature. The structural origin of the AT specificity at this point is unclear. However, the groove-binding ligand netropsin, which utilizes the same binding region of the fragment as the porphyrin (Lane et al., 1983) apparently excludes a G·C base pair from its interaction sequence through steric effects involving the 2-amino group of guanine (Kopka et al., 1985a,b). X-ray crystallographic analyses have shown that this group extends above the floor of the minor groove of DNA, and in the absence of hydrogen bond acceptor ability in the ligand (the case with both the porphyrin and netropsin), its presence discourages ligand binding. An additional factor explaining the AT specificity of the porphyrins may be related to electrostatic effects. Theoretical calculations on the electrostatic potential surface of DNA have shown that, although environmental effects can be a factor, the minor groove of AT sequences possesses a high negative potential (Weiner et al., 1982; Pullman 1983; Lavery & Pullman, 1985). Thus, in light of the tetracationic nature of the porphyrins the observed AT specificity may in part be due to electrostatic attractions between the porphyrins and the charged surface of DNA.

Inspection of Figures 4–9 reveals that the porphyrins cleave at all four possible nucleotide positions of DNA, strongly suggesting that the deoxyribose moiety is the primary site of attack in the strand scission process. This observation is consistent with the aforementioned activation properties of the metalloporphyrins (Groves & Nemo, 1983b) and the known DNA strand scission mechanisms of both Fe–bleomycin (Dabrowiak, 1983) and Fe–MPE (Hertzberg & Dervan, 1984).

Reaction of high-valent oxomanganese and oxoiron porphyrins with alkanes initially results in hydrogen abstraction from the alkane in the process leading to the formation of an alcohol. The parallels between this process and Fe–bleomycin-mediated hydrogen abstraction from deoxyribose (Giloni, 1981) suggests that the activated porphyrins may attack sites on the sugars, causing both cleavage of the ring and strand breakage. Interestingly, the nature of the scission chemistry may be dependent on the extent of DNA damage that takes place within a given site. Inspection of Figure 3 and the various densitometric scans, Figures 4–6, shows that as the amount of cleavage increases, oligomers possessing anomalous gel mobilities appear in the digests. These can be seen at positions 50, 61, 66, 67, and 90 for Fe–T4MPyP (Figure 8). Although further study is required, the modified DNA generated subsequent to the initial strand break may allow the porphyrin to attack the heterocyclic bases of DNA, which may in turn yield altered terminal chemistry. Recent studies with the dinucleotide dTdA and Fe–T4MPyP has shown that base modification in the presence of the activated porphyrin can in fact occur (Arakali et al., 1985).

Similarities between the porphyrins and Fe–bleomycin as well as Fe–MPE can also be found in the nature of the cleavage chemistry adjacent to the site of strand scission. Comparison of the electrophoretic mobilities of 3′-end-labeled oligomers produced from porphyrin and DNase I breakage of DNA revealed that the oligomers from both sources migrate with the same apparent mobility in the gel and thus may have the same terminal group, i.e. 5′-phosphate (Tapper & Clayton, 1981). A 5′-phosphate group also is adjacent to scission sites produced by both Fe–MPE (Hertzberg & Dervan, 1984) and Fe–bleomycin (Giloni, et al., 1981). Although Fe–bleomycin degradation of DNA is known to produce base 2-propenals, these cleavage products could not be chemically identified in

the porphyrin digests. In light of the known porphyrin activation chemistry, propenals may in fact be produced initially in the cleavage reaction. However, they could have been modified subsequently by further reaction with the activated porphyrin complex, to yield products that do not produce a chromogen in the presence of 2-thiobarbituric acid. This behavior, a negative test for base 2-propenals, is the same as that observed for Fe–MPE (Hertzberg & Dervan, 1984).

Figures 7 and 8 further reveal that Mn- and Fe–T4MPyP produce cleavage patterns that are asymmetric in nature and are unlike those of numerous DNA affinity cleaving agents examined by Dervan and co-workers (Schultz & Dervan, 1984). These agents, which exhibit high binding sequence specificities, report their positions on DNA by causing strand breakage adjacent to the site of binding. The breakage process involves activation of and radical release from an Fe–EDTA group attached via a flexible tether to a sequence-reading *N*-methylpyrrole peptide. The pattern of breaks on a given strand of DNA is symmetrically arranged over four to five nucleotides of the polymer. The breakage pattern is consistent with the Fe–EDTA group being located above the minor groove and releasing diffusable radical species, which react with the deoxyribose moieties of the polymer. The situation with the porphyrin, however, apears to be different. The compounds are rigid and likely to have a unique orientation within a given binding site on DNA. Since activation appears to take place on only the axial sites of the complex and contact between the substate and activated porphyrin is very likely important for reaction, the observed asymmetry in cleavage is not unexpected. A fixed arrangement of cleavage agent and DNA would permit only a limited number of DNA target sites to be attacked, conferring a degree of directionality to the strand scission process.

The observed cleavage specificity of Co–T4MPyP in the presence of ascorbate appears to be lower than that of the other two complexes (Figures 4–6 and 9). However, this may be due to the fact that the efficiency of breakage by this compound is low so that in order to obtain sufficient oligomer concentration for analysis it was necessary to increase the porphyrin to DNA base-pair ratio, r_t. Increases in r_t would ultimately cause population of lower affinity sites on the fragment, which would in turn appear as cleavage sites in the analysis. Alternatively, a change in mechanism in which the axial positions of the metal are not actively involved in the strand scission process also accounts for this. A comparison of Mn–, Fe–, and Co–T4MPyP scission of the fragment in the presence of ascorbate (Figure 4) shows most dramatically that in the position 150 region, Mn and Fe cut adjacent to position 150 while Co cuts between. This may be expected if in the reaction of Co-T4MPyP and ascorbate a diffusable radical is formed which nicks at sites away from the porphyrin binding site. This behavior was not observed for superoxide or iodosobenzene activation with Co–T4MPyP. In these cases the similarity between Co–T4MPyP cutting specificity and that for the Fe and Mn compounds suggests that the Co axial sites may be intimately involved in the strand scission process.

The metalloporphyrins have potential for studying ligand–DNA interactions by using footprinting methodology. While it is true that they cleave DNA with a high degree of AT specificity and thus cannot be directly used to report ligation events in GC-rich regions of the polymer, many groove-binding ligands, e.g. netropsin, distamycin, and the "lexitropsins" have binding sites in common with the porphyrins (Lane et al., 1983, 1985; Lown et al., 1986b). Thus, it should be possible to use these metalloporphyrins as selective footprinting probes for ligands having AT binding specificity. Since the DNA cleavage mechanism for the porphyrins appears to be different than that for the enzyme DNase I, and in certain respects Fe–MPE, it will be important to quantitatively analyze the binding information reported by all three probes. This will allow an assessment of whether and to what extent a given probe disturbs the ligand–DNA equilibrium and ultimately which probes will be useful in evaluating ligand binding constants from footprinting data (Goodisman & Dabrowiak, 1985). Noteworthy, in the case of the porphyrins, is that the level of porphyrin required for successful analysis of footprinting digests is about 2 orders of magnitude less than that typically used for Fe–MPE (Hertzberg & Dervan, 1984). How the presence of reduced amounts of cleavage agents affects the ligand–DNA equilibrium in a footprinting experiment remains to be evaluated.

Finally, the cationic porphyrins possess significant potential as "DNA-reporter" ligands. They are ridged structures and when bound to DNA are likely to have a preferred orientation on the polymer. In light of the fact that the catalytic properties are highly directional in nature, strand scission events could be used to monitor local changes in DNA structure induced by the binding of other ligands adjacent to the porphyrins. It is suspected that structural changes propagated through the polymer are the basis for allosteric effects associated with drug binding to DNA (Krugh & Young, 1977).

Registry No. MnT4MPyP, 70649-54-6; FeT4MPyP, 60489-13-6; CoT4MPyP, 51329-41-0; $O_2^{\bullet-}$, 11062-77-4; IOPh, 536-80-1; ascorbate, 50-81-7.

REFERENCES

Arakali, A. V., Byrnes, R., & Fiel, R. J. (1985) *Book of Abstracts. Fourth Conversation in Biomolecular Stereodynamics*, pp 137–138, Adenine, Guilderland, NY.

Barton, J. K. (1985) *Comments Inorg. Chem. 3*, 321–348.

Barton, J. K., & Raphael, A. L. (1982) *J. Am. Chem. Soc. 106*, 2466.

Barton, J. K., & Raphael, A. L. (1985) *Proc. Natl. Acad. Sci. U.S.A. 82*, 6460–6464.

Behe, M., & Felsenfeld, G. (1981) *Proc. Natl. Acad. Sci. U.S.A. 78*, 1619–1623.

Dabrowiak, J. C. (1982) *Adv. Inorg. Biochem. 4*, 69–113.

Dabrowiak, J. C., Skorobogaty, A., Rich, N., Vary, C. P. H., & Vournakis, J. N. (1986) *Nucleic Acids Res. 14*, 489–499.

Eichhorn, G. L. (1973) in *Inorganic Biochemistry* (Eichhorn, G. L., Ed.) Vol. 2, p 1191–1243, Elsevier, New York.

Eichhorn, G. L., & Marzilli, L. G. (1981) *Adv. Inorg. Biochem. 3*, 1.

Fazakerly, G. V. (1984) *Nucleic Acids Res. 12*, 3643–3657.

Fiel, R. J., Beerman, T. A., Mark, E. H., & Datta-Gupta, N. (1982) *Biochem. Biophys. Res. Commun. 107*, 1067–1074.

Fiel, R. J., Carvlin, M. J., Byrnes, R. W., & Mark, E. H. (1985) in *Molecular Basis of Cancer, Part B: Macromolecular, Recognition, Chemotherapy, and Immunology* (Rein, R., Ed.) pp 215–226, Alan R. Liss, New York.

Fontecave, M., & Mansuy, D. (1984) *Tetrahedron 40*, 4297–4311.

Gessner, R. V., Quigley, G. J., Wang, A. H.-J. van der Marel, A., van Boom, J. H., & Rich, A. (1985) *Biochemistry 24*, 237–240.

Giloni, L., Takashita, M., Johnson, F., Iden, C., & Grollman, A. P. (1981) *J. Biol. Chem. 256*, 8608–8615.

Goodisman, J., & Dabrowiak, J. C. (1985) *J. Biomol. Struct. Dyn. 2*, 967–979.

Groves, J. T. (1979) *Adv. Inorg. Biochem. 1*, 119–145.

Groves, J. T., & Nemo, T. E. (1983a) *J. Am. Chem. Soc. 105*, 5786–5791.
Groves, J. T., & Nemo, T. E. (1983b) *J. Am. Chem. Soc. 105*, 6243–6248.
Groves, J. T., Haushalter, R. C., Nakamura, M., Nemo, T. E., & Evans, B. J. (1981) *J. Am. Chem. Soc. 103*, 2884–2886.
Groves, J. T., Watanabe, J., & McMurry, T. J. (1983) *J. Am. Chem. Soc. 105*, 4489–4490.
Harris, F. L., & Toppen, D. L. (1978) *Inorg. Chem. 17*, 71.
Hertzberg, R. P., & Dervan, P. B. (1984) *Biochemistry 23*, 3934–3945.
Kelly, J. M., Murphy, M. J., McConnell, D. J., & OhUigin, C. (1985) *Nucleic Acids Res. 13*, 167–184.
Kopka, M. L., Yoon, C., Goodsell, D., Pjura P., & Dickerson, R. E. (1985a) *Proc. Natl. Acad. Sci. U.S.A. 82*, 1376–1380.
Kopka, M. L., Yoon, C., Goodsell, D., Pjura, P., & Dickerson, R. E. (1985b) *J. Mol. Biol. 183*, 553–563.
Krugh, T. R., & Young, M. A. (1977) *Nature (London) 267*, 627.
Lane, M. J., Dabrowiak, J. C., & Vournakis, J. N. (1983) *Proc. Natl. Acad. Sci. U.S.A. 80*, 2360–2364.
Lane, M. J., Vournakis, J. N., & Dabrowiak, J. C. (1985) in *Molecular Basis of Cancer, Part B: Macromolecular Recognition, Chemotherapy and Immunology* (Rein, R., Ed.) pp 145–153, Alan R. Liss, New York.
Lavery, R., & Pullman, B. (1985) *J. Biomol. Struct. Dyn. 2*, 1021–1032.
Lown, J. W., Sondhi, S. M., Org. C.-W., Skorobogaty, A., Kishikawa, H., & Dabrowiak, J. C. (1986a) *Biochemistry 25*, 5111–5117.
Lown, J. W., Krowicki, K., Bhat, U. G., Skorobogaty, A., Ward, B., & Dabrowiak, J. C. (1986b) *Biochemistry* (in press).
Maniatis, T., Fritsch, E. T., & Sambrook, J. (1982) *Molecular Cloning—A Laboratory Manual*, pp 150–185 and 458–472, Cold Spring Harbor Laboratory, Cold Spring Harbor, NY.
Pasternack, R. F., Gibbs, E. J., & Villafranca, J. J. (1983a) *Biochemistry 22*, 5409–5417.
Pasternack, R. F., Gibbs, E. J. & Villafranca, J. J. (1983b) *Biochemistry 22*, 2406–2414.
Pasternack, R. T., Autebi, A., Ehrlich, B., & Sidney, D. (1984) *J. Mol. Catal. 23*, 235–242.
Peretz, P., Soloman, D., Weinraub, D., & Farraggi, M. (1982) *Int. J. Radiat. Biol. Relat. Stud. Phys., Chem. Med. 42*, 449–456.
Peterson, J. A., Ishimura, Y. Baron, J., & Estabrook, R. W. (1973) in *Oxidases and Related Redox Systems* (King, T. E., Mason, H. S., & Morrison, M., Eds.) p 565, University Park Press, Baltimore, MD.
Pullman, B. (1983), *J. Biomol. Struct. Dyn. 1*, 773–794.
Schultz, P. G., & Dervan, P. B. (1984) *J. Biomol. Struct. Dyn. 1*, 1133–1147.
Spassky, A., & Sigman, D. S. (1985) *Biochemistry 24*, 8050–8056.
Tapper, D. P, & Clayton, D. A. (1981) *Nucleic Acids Res. 9*, 6787–6794.
Traylor, T. G., Lee, W. A., & Stynes, D. V. (1984a) *Tetrahedron 40*, 553–568.
Traylor, T. G., Lee, W. A., & Stynes, D. V. (1984b) *J. Am. Chem. Soc. 106*, 755–764.
Van Dyke, M. W., Hertzberg, R. P., & Dervan, P. B. (1982) *Proc. Natl. Acad. Sci. U.S.A. 79*, 5470–5474.
Ward, B., Skorobogaty, A., & Dabrowiak, J. C. (1986) *Biochemistry* (in press).
Weiner, P. K., Langraidge, R., Blaney, J. M., Schaefer, R., & Kollman, P. A. (1982) *Proc. Natl. Acad. Sci. U.S.A. 79*, 3754–3758.
Woisard, A., Fazakerly, V., & Guschelbauer, W. (1985) *J. Biomol. Struct. Dyn. 2*, 1205–1220.